

# Recent results from the UrQMD hybrid model for heavy ion collisions

Marcus Bleicher, Stephan Endres, Jan Steinheimer, Hendrik van Hees

*Frankfurt Institute for Advanced Studies (FIAS), Ruth-Moufang-Strasse  
1, 60438 Frankfurt am Main, Germany*

*Institut für Theoretische Physik, Johann-Wolfgang-Goethe-Universität,  
Max-von-Laue-Strasse 1, 60438 Frankfurt am Main, Germany*

## Abstract

These proceedings present recent results from transport-hydrodynamics-hybrid models for heavy ion collisions at relativistic energies. The main focus is on the absorption of (anti-)protons in the hadronic afterburner stage of the reaction, di-lepton production at SPS and heavy quark dynamics.

## 1. Introduction

A major theme in todays high energy heavy ion physics is to explore the phases of Quantum Chromodynamics (QCD) at very high densities and temperatures. To connect ab-initio information on the properties of QCD-matter, e.g., the Equation of State (EoS) or transport coefficients like the viscosities with experimentally observable quantities one has to rely on transport approaches that describe the time evolution of the hot and dense matter created until the system has ceased to interact. Transport models and hydrodynamic approaches have a long tradition in providing this link. Unfortunately, the areas of application of both approaches seems mutually exclusive: Boltzmann equation based transport simulations are well suited for the less dense stages of the reaction or for lower energies, while hydrodynamic simulations are only justified

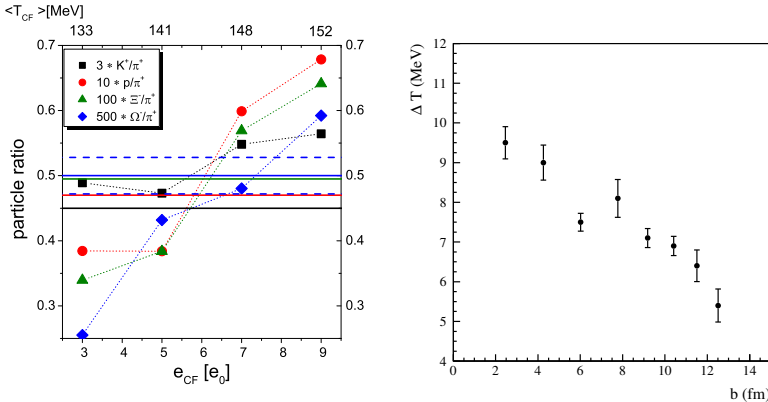


Fig. 1: Left: Modification of the final particle ratios as a function of the transition energy density  $\epsilon_{CF}$  for the Cooper-Frye prescription in Pb+Pb collisions at  $\sqrt{s_{NN}} = 2.76$  TeV [13]. Right: Corrected temperature of the freeze-out points on the phase diagram [15, 16].

during the most dense stages of the reaction's evolution or at very high collision energies.

## 2. Model description

For the present studies we use the UrQMD model v3.3 in hybrid mode [1–3]. This model couples the fluctuating initial state [4] generated event-by-event by the hadron and string dynamics from UrQMD to an ideal hydrodynamic evolution. For the evolution of the hydrodynamic part different equations of state can be applied, including a hadron gas EoS and a chiral EoS with a transition to a quark-gluon plasma. At the end of the hydrodynamic evolution, defined by a transition energy density, the hydrodynamic cells are converted to particles with a Cooper-Frye prescription [5], and the decoupling stage is handled by the UrQMD hadronic cascade [6]. For similar approaches by other groups we refer to [7–12] and references therein.

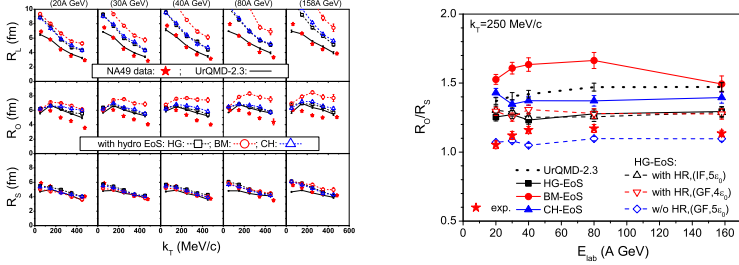


Fig. 2: Left: HBT radii for different beam energies as a function of the transverse momentum of the pion pair for different equations of state [17]. Right: Ratios of the out to side radii as function of beam energy and for different equations of state [17].

### 3. Matter and Antimatter

The effect of the hadronic afterburner can be seen directly in the yields of the protons and anti-protons in nuclear collisions at the LHC. Fig.1 (left) shows the modifications of the particle yields due to the hadronic corona as a function of the energy density at which the Cooper-Frye particlization is applied. One observes that for realistic transition energy densities around  $\epsilon_{CF} = 5\epsilon_0$  the proton and anti-proton yields are reduced by approximately 50% in line with the observed values at the LHC [13]. A similar conclusion is also reached if the back reaction  $5\pi \rightarrow p\bar{p}$  is included [14]. The systematic error, if the back reaction is neglected is on the order of 10% [14]. Fig. 1 (right) shows the temperatures extracted from chemical fits for different centralities in Pb+Pb reactions at  $\sqrt{s_{NN}} = 2.76$  TeV. The temperature differences  $\Delta T$  are obtained from the temperature differences between uncorrected fits and ‘corrected’ fits (i.e., corrected for baryon absorption in the hadronic corona as given by UrQMD) to the model data [15, 16].

### 4. Hanbury-Brown–Twiss Correlations

Let us next explore the effect of different equations of state. One expects that a phase transition to a quark-gluon plasma (and back to the hadron gas) should result in a delay of the expansion of the system depending on

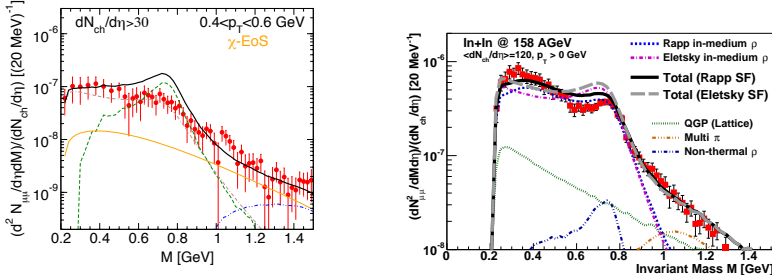


Fig. 3: Left: Di-muon spectrum for In+In collisions at 160 AGeV from hybrid-model simulations [18] in comparison to NA60 data [19]. Right: Di-muon spectrum for In+In collisions at 160 AGeV from coarse grained simulations in comparison to NA60 data [19]. Calculations with the Rapp-Wambach and Eletsky spectral functions are compared [24].

the magnitude of the latent heat. To explore this effect we compare hybrid simulations for different equations of state using Hanbury-Brown-Twiss (HBT) correlations [17]. Fig. 2 (left) provides a comparison of various equations of state (hadron gas EoS, chiral EoS, bag model EoS, and a pure UrQMD cascade simulation). One observes that the pure UrQMD simulation, the hadron gas EoS and the chiral EoS provide a reasonable description of the data, while the bag model EoS clearly overshoots the data. The data and the simulations are summarized in Fig. 2 (right) for the  $R_{\text{out}}/R_{\text{side}}$  ratio for different beam energies. Here one clearly observes the expected maximum in the life time of the system in case of the bag model EoS. However, the data seem to favor a transition with a small latent heat without a substantial time delay as provided by the hadron gas EoS and the chiral EoS.

## 5. Dileptons

As a next step let us investigate the temperature and density evolution with penetrating probes. To this aim we compare coarse-grained transport simulations to hybrid-model calculations to explore differences due to the assumption of local equilibration and due to different spectral functions. Fig. 3 left shows the hybrid-model calculation [18] (Eletsky

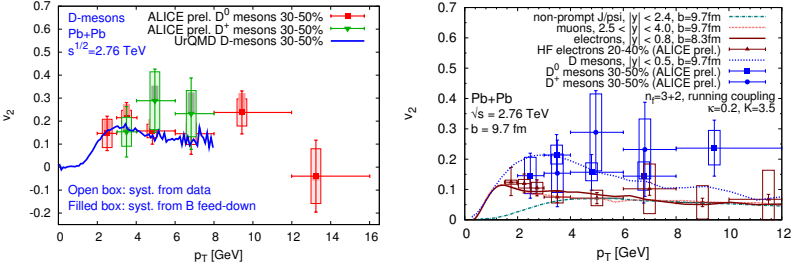


Fig. 4:  $\text{Pb}+\text{Pb}$  reactions at  $\sqrt{s_{NN}} = 2.76$  TeV. Models compared to ALICE data [27]. Left: Hybrid model calculations with a Langevin treatment of the heavy quark dynamics [25]. Right: Parton cascade calculation. Figure taken from [26].

spectral function) for dimuon production in In+In reactions in comparison to the NA60 data [19]. One observes that the hybrid model provides a good description of the experimental data, however with a slight overestimation of the yield around the  $\rho$  peak. We compare this to the coarse-grained transport simulation [20] in Fig. 3 (right). In this case we show in addition a comparison to the Rapp-Wambach spectral function [21–23]. Generally we observe a very good description of the NA60 data [19]. The main differences between both approaches seem to be caused by the different spectral functions, with the Rapp-Wambach spectral function providing a better description of the data. The hybrid-model results also show an excess above the data of the  $\rho$  around its pole mass. This mainly stems from the initial and final stage which are handled by the hadronic cascade and where (in contrast to the hydrodynamic phase) no explicit medium modifications of the spectral shape are considered.

## 6. Charm

An alternative way to explore the properties of the created matter is to investigate its transport properties in terms of drag and diffusion coefficients. To this aim we model the propagation of heavy quarks, i.e., charm quarks through the matter created in the hybrid approach. In Fig. 4 we compare the results for the  $D$ -meson elliptic flow  $v_2$  in

Pb+Pb collisions at the LHC based on the hybrid model [25] (left figure) with the results obtained from a recent parton cascade [26] study (right figure). For both cases we observe a similar quality for the description of the experimental data. This indicates that the density and temperature distribution and evolution in the hybrid approach and the parton cascade approach seem to be very similar. This may indicate that a substantial amount of local equilibrium is achieved in such collision as the dynamics of the heavy quarks does not seem to depend on the details of the system evolution.

## 7. Summary

In summary, hybrid models combining a hydrodynamic simulation for the hot and dense stages of the reaction coupled to Boltzmann dynamics for the early and late stage of the evolution provide an excellent tool to investigate the properties of QCD matter created at SPS, RHIC and LHC. For these proceedings we have discussed the modifications of the (anti-)proton yields due to absorption effects in the final state hadronic afterburner. We have then explored the temperature and density evolution by means of dilepton radiation and charm dynamics. In comparison to available data and alternative approaches, we concluded that the hybrid approach provides a reliable and sensible basis for these investigations.

## 8. Acknowledgements

M. B. wants to thank the organizers for an excellent meeting and many fruitful and stimulating discussions. This work has been supported by the Hessian LOEWE initiative through HIC for FAIR.

1. S. A. Bass *et al.*, Prog. Part. Nucl. Phys. **41**, 255 (1998) [Prog. Part. Nucl. Phys. **41**, 225 (1998)] [[arXiv:nucl-th/9803035](#)].
2. M. Bleicher *et al.*, J. Phys. **G25**, 1859 (1999) [[arXiv:hep-ph/9909407](#)].
3. H. Petersen, J. Steinheimer, G. Burau, M. Bleicher and H. Stocker, Phys. Rev. C **78**, 044901 (2008) [[arXiv:0806.1695 \[nucl-th\]](#)].

---



---

4. M. Bleicher *et al.*, Nucl. Phys. A **638**, 391 (1998).
5. P. Huovinen and H. Petersen, arXiv:1206.3371 [nucl-th].
6. F. Becattini, M. Bleicher, T. Kollegger, M. Mitrovski, T. Schuster and R. Stock, Phys. Rev. C **85**, 044921 (2012) [arXiv:1201.6349 [nucl-th]].
7. V. K. Magas, L. P. Csernai and D. Strottman, Nucl. Phys. A **712**, 167 (2002) [arXiv:hep-ph/0202085].
8. L. P. Csernai, V. K. Magas, E. Molnar, A. Nyiri and K. Tamosiunas, Eur. Phys. J. A **25**, 65 (2005) [arXiv:hep-ph/0505228].
9. R. Andrade, F. Grassi, Y. Hama, T. Kodama, O. . J. Socolowski and B. Tavares, Eur. Phys. J. A **29**, 23 (2006) [arXiv:nucl-th/0511021].
10. T. Hirano and M. Gyulassy, Nucl. Phys. A **769**, 71 (2006) [arXiv:nucl-th/0506049].
11. C. Nonaka and S. A. Bass, Nucl. Phys. A **774**, 873 (2006) [arXiv:nucl-th/0510038].
12. K. Werner, I. Karpenko, T. Pierog, M. Bleicher and K. Mikhailov, Phys. Rev. C **82**, 044904 (2010) [arXiv:1004.0805 [nucl-th]].
13. J. Steinheimer, J. Aichelin and M. Bleicher, Phys. Rev. Lett. **110**, 042501 (2013) [arXiv:1203.5302 [nucl-th]].
14. Y. Pan and S. Pratt, Phys. Rev. C **89** (2014) 4, 044911.
15. F. Becattini, M. Bleicher, T. Kollegger, T. Schuster, J. Steinheimer and R. Stock, arXiv:1212.2431 [nucl-th].
16. F. Becattini, E. Grossi, M. Bleicher, J. Steinheimer and R. Stock, Phys. Rev. C **90** (2014) 5, 054907 [arXiv:1405.0710 [nucl-th]].
17. Q. f. Li, J. Steinheimer, H. Petersen, M. Bleicher and H. Stocker, Phys. Lett. B **674**, 111 (2009) [arXiv:0812.0375 [nucl-th]].
18. E. Santini, J. Steinheimer, M. Bleicher and S. Schramm, Phys. Rev. C **84**, 014901 (2011) [arXiv:1102.4574 [nucl-th]].
19. R. Arnaldi *et al.* [NA60 Collaboration], Eur. Phys. J. C **61**, 711 (2009) [arXiv:0812.3053 [nucl-ex]].
20. S. Endres, H. van Hees, J. Weil and M. Bleicher, arXiv:1412.1965 [nucl-th].
21. R. Rapp, J. Wambach, Eur. Phys. J. A **6**, 415 (1999).
22. R. Rapp and J. Wambach, Adv. Nucl. Phys. **25**, 1 (2000) [arXiv:hep-ph/9909229].
23. H. van Hees and R. Rapp, Phys. Rev. Lett. **97** (2006) 102301 [hep-ph/0603084].
24. S. Endres, H. van Hees, J. Weil and M. Bleicher, arXiv:1502.01948 [nucl-th].
25. T. Lang, H. van Hees, J. Steinheimer and M. Bleicher, arXiv:1211.6912 [hep-ph].
26. J. Uphoff, O. Fochler, Z. Xu and C. Greiner, Nucl. Phys. A **910-911**, 401 (2013) [arXiv:1208.1970 [hep-ph]].
27. G. Ortona [ALICE Collaboration], arXiv:1207.7239 [nucl-ex].